REACTIVE TRANSPORT MODELING OF AMD RELEASE AND ATTENUATION AT THE FAULT LAKE TAILINGS AREA, FALCONBRIDGE, ONTARIO[1]

Connie G. Romano[2], K. Ulrich Mayer, and David W. Blowes

Abstract. Numerical simulations of the Fault Lake Tailings were conducted to assess the long-term impact of AMD-generation on downgradient receptors. The effects of impoundment geometry, contrasting permeability, water content, and mineralogy of tailings and native sediments were considered. Simulation results suggest that over a time period of 1,000 years only the top three meters of tailings become oxidized and that AMD is preferentially released at the periphery of the impoundment. Although the permeability of the tailings is lower than that of the aquifer and groundwater flow is deflected around the deep saturated tailings mass, AMD is not inhibited from percolating into the aquifer, because the bulk of the tailings are located within the vadose zone. The carbonate content of the underlying material likely provides sufficient buffering capacity to attenuate most metals and neutralize pH over the long-term.

Additional Key Words: sulfide mineral oxidation, porous envelope effect, mass loading, sensitive receptor

[1] Paper presented at the 7th International Conference on Acid Rock Drainage (ICARD), March 26-30, 2006, St. Louis MO. R.I. Barnhisel (ed.) Published by the American Society of Mining and Reclamation (ASMR), 3134 Montavesta Road, Lexington, KY 40502

[2]Connie G. Romano, Senior Hydrogeologist, Golder Associates, 500 – 4260 Still Creek Drive, Burnaby, BC, V5C 6C6, Canada. K. Ulrich Mayer, Assistant Professor of Hydrogeology, University of British Columbia, Dept. of Earth and Ocean Sciences, 6339 Stores Rd., Vancouver, BC, V6T 1Z4, Canada. David, W. Blowes, Professor of Geochemistry, University of Waterloo, Dept. of Earth Sciences, 200 University Ave. W., Waterloo, ON, N2L 3G1, Canada.

7th International Conference on Acid Rock Drainage, 2006 pp 1673- 1693
DOI: 10.21000/JASMR06021673

https://doi.org/10.21000/JASMR06021673

Introduction

At the Fault Lake Tailings area, sulfide minerals contained in the tailings mass have been exposed to atmospheric O_2, resulting in the generation of acidic groundwater with high Fe, SO_4^{-2}, Ni, and Cu concentrations. The rate of oxidation was greatest immediately after tailings deposition ceased in 1978 (NTC 1995) and has been decreasing over time. To date, only minor contamination has been identified downgradient of the tailings area (Golder 1996). Although difficult to predict, the long term impact of the Fault Lake Tailings Area on the surrounding subsurface environment and on the downgradient sensitive receptors is of great interest to Falconbridge and the Ministry of Northern Development and Mines. The downgradient sensitive receptor considered here is the nearest of several small lakes found approximately one kilometer to the northeast of the tailings area. Prediction of this impact is problematic because of the complexity of geochemical reactions affecting acid neutralization and metal mobility in the thick unsaturated zone and in the underlying aquifer, and the limited physical and geochemical data available for the surrounding overburden deposits. The objective of this paper is to obtain additional insight into the transient release and attenuation of acid mine drainage (AMD) at this site through the application of a multi-component reactive transport model (MIN3P) which uses a fully integrated approach to simulating groundwater flow, contaminant transport, and geochemical interactions in variably-saturated porous media. This code has previously been used to investigate AMD generation, attenuation, and remediation (Mayer et al., 1999, Mayer et al., 2000, Bain et al., 2001, Mayer et al., 2002, Amos et al., 2004, Jurjovec et al., 2004); however, this study is the first large scale 2D-application taking into account site geometry.

Hydrogeological and Geochemical Setting

The Fault Lake Tailings Area is situated near the Town of Falconbridge, approximately 18 km northeast of Sudbury, Ontario. As described by NTC (1995) and Golder (1996), approximately 5.7 million tonnes of tailings were deposited in the Fault Lake Tailings Area over a 14-year period from 1964 to 1978. The tailings impoundment was established in a closed depression formed around a former kettle lake ('kettle' refers to a depression caused by glacial processes). This lake is one of a series of kettle lakes located at the eastern edge of an extensive esker (Fig. 1). The base of the tailings deposit is shaped such that its depth varies from zero at the perimeter of the facility to a maximum of approximately 38 m near its center. The water table is about 22 m below the tailings surface, and only a limited area of the tailings extends below the water table. The bulk of the tailings, therefore, are unsaturated.

Infiltration on the north side of the impoundment ultimately contributes to groundwater flowing to the northeast along the esker, and infiltration on the south side ultimately contributes to groundwater flowing southward towards the New Tailings Area (Fig. 2). Only the north side of the impoundment and the associated downgradient environment to the northeast is evaluated in this study. The tailings contain up to 22 vol. % (50 wt. %) sulfide minerals. Ninety-eight percent of the sulfide minerals are pyrrhotite, the remaining 2 vol. % consist mostly of chalcopyrite, pentlandite, and trace amounts of pyrite (Golder 1996). Other primary mineral phases present include small amounts of magnetite, quartz and aluminosilicate minerals (significant chlorite content and minor plagioclase feldspar content). The unoxidized tailings material also contain minor amounts of carbonate, mica, and amphibole minerals.

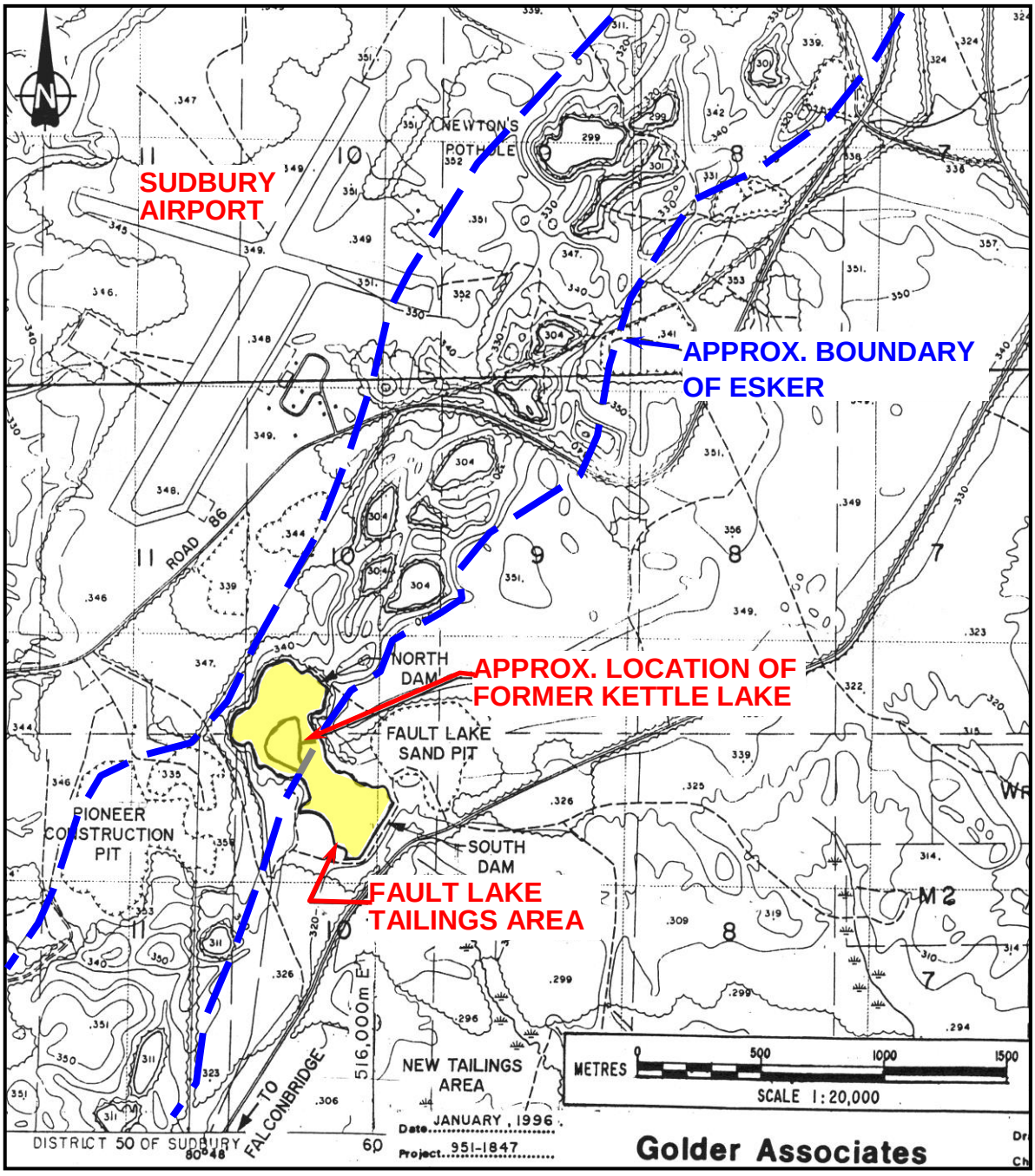

Figure 1: Fault Lake Tailings Area

The tailings were produced from the milling and concentrating of nickel ore in the Falconbridge smelter complex, located about 3.5 km south-southwest of the impoundment. The tailings are generally stratified into three layers, varing primarily with respect to sulfide content. The basal layer, on average 10 m thick, is pyrrhotite poor (approximately 1 vol. % pyrrhotite) and is termed 'Low S Tailings', the top layer, on average 5 m thick, is pyrrhotite rich (up to 22 vol. % pyrrhotite) and is termed 'High S Tailings', and the middle layer (approximately 5 vol. %

pyrrhotite), on average 5 m thick, is a transition between the high and low sulfide layers, and is referred herein as 'Blended Tailings'. This results in a structure where the top layer of the tailings, which is most accessible to atmospheric O_2, generally has the highest sulfide mineral content.

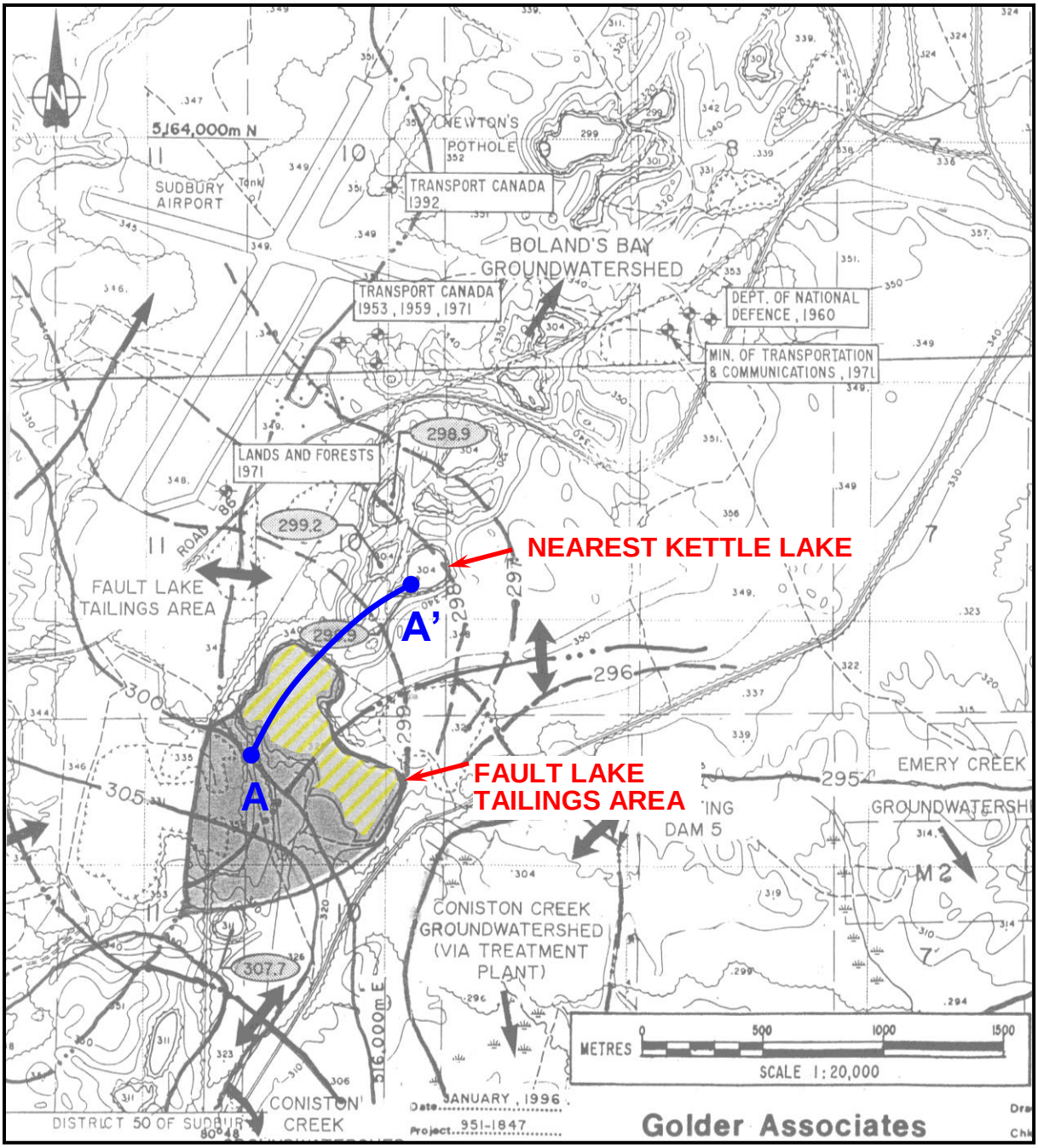

Figure 2: Regional Groundwater Flow Regime and Trajectory of the 2D Cross-Section. [Modified from Golder (1996). Shaded area denotes groundwater recharge area for Fault Lake Tailings Area. Piezometric contours in 5 m intervals.]

The overburden deposits beneath and surrounding the north half of the tailings impoundment are predominantly eskerine deposits, typically consisting of coarse-grained sand and gravel with cobbles and boulders. These deposits characterize the aquifer underlying the tailings. Due to the absence of mineralogical data for these deposits, their composition was approximated by data obtained by Golder (1998b) for native sediments from the East Mine Tailings Area, located approximately 2 km east of the Fault Lake Tailings Area. The native sediments have up to 65 vol. % quartz. Other primary mineral phases present in the sediments include aluminosilicates such as plagioclase and alkali feldspars, and trace amounts of calcite, sulfide minerals (chalcopyrite, pyrite, and pyrrhotite), oxides, and clay minerals. The overburden thickness, including the tailings deposit, varies within the study area from 36 m to more than 60 m.

Summary of Conceptual Model

The primary mechanisms considered to cause AMD generation, heavy metal contamination, and heavy metal attenuation at the Fault Lake Tailings Area are presented below. These are primarily based upon field observations, qualitative mineralogical studies and elemental analyses of the tailings. The conceptual model also includes several mineral phases which were noted in previous field and modeling studies of the nearby Nickel Rim Mine Tailings near Sudbury, Ontario (Johnson et al., 2000, Mayer et al., 2002). These tailings are qualitatively similar to the composition of Fault Lake Tailings.

Elevated Fe, Ni and SO_4^{-2} concentrations are primarily due to the oxidation of Ni-bearing pyrrhotite [$(Fe,Ni)_{1-x}S$]. The generation of acidity by the oxidation of pyrrhotite by O_2 is dependent on the ratio between Fe/Ni and S in this mineral. Fractions of chalcopyrite and pentlandite are also contained in the tailings. Cu and Ni are released to the pore water when these minerals oxidize. Oxidation of sulfide minerals and Fe^{+2} in the vadose zone is accompanied by the precipitation of ferric oxyhydroxides and ferric hydroxysulfates such as ferrihydrite and jarosite (Johnson et. al, 2000). The precipitation of these secondary minerals leads to the attenuation of Fe and SO_4^{-2}, but releases additional H^+.

The low pH-water causes the dissolution of minerals capable of pH-buffering. The results of mineralogical (qualitative XRD) analyses and acid neutralization tests of the tailings solids, presented by NTC (1995), suggest that unaltered tailings material contains a fair amount of carbonate minerals, here assumed to be present as calcite. Acidity in the tailings water also enhances the dissolution of aluminosilicate minerals, which may provide additional acid neutralization. A variety of aluminosilicates are present in the tailings. In this study, only the phases exhibiting relatively rapid reaction kinetics are considered, namely chlorite, anorthite, and mica, represented by biotite.

Oxidation of sulfide minerals and dissolution of pH-buffering mineral phases may cause the precipitation of a number of additional secondary mineral phases including siderite, amorphous Al-hydroxide, gypsum and amorphous silica. Siderite, amorphous Al-hydroxide, ferrihydrite, and jarosite may also redissolve, providing additional pH-buffering capacity, but simultaneously releasing metals (Johnson et. al, 2000). Gypsum and amorphous silica control aqueous concentrations of Ca, SO_4^{-2} and Si.

Dissolved Cu concentrations at the Fault Lake Tailings Area are near or below the detection limit of 0.025 mg/L. This may be attributed to the incomplete oxidation of sulfides and the

consumption of Fe^{+3} in the oxygen-depleted portion of the tailings, which may create conditions that favour the precipitation of covellite (Johnson et. al, 2000).

Dissolved Ni concentrations at the Fault Lake Tailings Area do not persist far below the zone of oxidation. The mechanism for the Ni attenuation at this site is not known. It is speculated that Ni may be co-precipitating with secondary ferric hydroxides or undergo sorption, but this process is difficult to quantify. The attenuation of Ni as $Ni(OH)_2$ (am) is unlikely, under the expected pH conditions in the tailings and aquifer materials. Mineralogical analyses would be required to determine the composition of the secondary phases and to identify the mechanisms leading to the attenuation of Ni.

Application of MIN3P Model

Both one-dimensional and two-dimensional simulations were performed using the multicomponent reactive transport code MIN3P (Mayer et al., 2002). These simulations considered an exposed tailings surface, aqueous and gaseous mass transport, sulfide mineral oxidation in the tailings, and pH-buffering reactions, as described in the conceptual model. The 1D vertical simulations were conducted to assess the validity of the conceptual model through a comparison of observed versus computed chemical concentrations along a vertical profile through the centre and thickest part of tailings area. The 2D cross-sectional simulation was built on the results of the 1D simulations. This simulation was used to investigate the effect of the 2D-flow field on the movement of the major constituents in the tailings drainage plume (pH, Fe, SO_4^{-2}, Ni, and Cu) and to evaluate the impact of the tailings impoundment on the surrounding subsurface environment (particularly the underlying aquifer) and on the downgradient sensitive receptor, the nearest kettle lakes.

An active non-hazardous waste landfill and an active land farm for remediation hydrocarbon-contaminated soil partially cover the tailings surface. In much of the areas of the landfill, it is underlain by a multi-layer soil cover comprised of 0.3 m thick gravel overlying 0.6 m thick compacted clayey soil. The basal layer of the land farm consists of a HDPE geomembrane supported on and covered by sand layers. The remaining tailings area is covered by a 0.6 m thick gravel layer. Although these soil covers were placed over the tailings between 1997 and 2000, their influence on AMD generation is not considered in the simulations because of the long time frame of this investigation (model simulations to 1,000 years) relative to the expected lifespan of the covers (i.e., the potential decline in the integrity of surface covers due frost heave, desiccation cracks, rootholes, erosion, etc.), and the lack of cover performance data (e.g., infiltration and O_2 flux through the covers). Therefore, this study provides a conservative estimate with respect to infiltration, oxygen influx, and AMD generation.

Model Input Parameters

The physical parameters used to represent the eskerine aquifer and the tailings are presented in Table 1, along with their respective source information. These parameters are based on measured properties, where available, or were estimated from existing information and literature data. A uniform isotropic hydraulic conductivity was assigned to the tailings mass. Using this approach, we were able to obtain a good agreement between the 1D simulation results and the observed pore water concentrations along a vertical profile at the centre of the tailings impoundment. This was possible despite the fact that the real system will likely exhibit some degree of anisotropy and heterogeneity induced by the process of tailings deposition. Of special

note is that water saturations of approximately 60% were assumed to adequately represent average moisture conditions for all unsaturated tailings. These saturations provide a good fit between observed and simulated O_2 partial pressures in the shallow tailings (see 1D results below). This assumption was necessary because the measured volumetric moisture content data for unsaturated tailings (NTC 1995) were limited to only the top 2.5 m of tailings and varied over a wide range (30-76%). This assumption is crucial with respect to the potential for the release of acidity and metals from the tailings, because the ingress of atmospheric oxygen increases strongly (superlinearly) with decreasing moisture content. Van Genuchten-soil hydraulic function parameters and residual water contents were adjusted to obtain the assumed water saturations in the unsaturated tailings.

The mineral volume fractions used to represent the composition of reactive solids in the tailings and aquifer are presented in Table 2, along with their source information and derivations. The results of acid neutralization tests of the tailings solids by NTC (1995) (reported as neutralization potential (NP) in units of kg of $CaCO_3$/tonne of solids) were directly used to estimate the calcite content in the unaltered tailings (Blended and Low S Tailings). It was assumed that the measured NP is representative of carbonate content, because reaction kinetics of silicate dissolution are slow. The calcite content in the High S Tailings was partially depleted due to sulfide mineral oxidation reactions at the tailings surface; therefore, the initial calcite content was determined by model calibration (3 vol%).

The reaction rates related to the oxidation of pyrrhotite, pentlandite, and chalcopyrite were modeled using effective rate constants, which are lumped parameters defined as the products of the surface area normalized rate constants and the reactive surface area. A constant effective oxidation rate constant was used for pyrrhotite, whereas for pentlandite and chalcopyrite, a first order rate with respect to oxygen was applied. Rapid oxidation kinetics were assumed to produce the sharp oxidation front observed in the field (NTC, 1995). The pH-dependent rate expressions related to the dissolution of anorthite, biotite, and chlorite use lab-derived rate constants, require a reactive surface area, and are fractional-order with respect to H^+. The estimated reactive surface area of these minerals, presented in Table 2, were calculated from the median grain size (d50) and mineral content of the tailings, and assuming that the mineral grains are perfectly spherical.

All kinetically-controlled reactions, *i.e*. sulfide mineral oxidation and silicate mineral dissolution reactions described above, are treated as surface-controlled reactions. All other reactions, *i.e.* calcite dissolution, secondary mineral precipitation and dissolution, are treated as quasi-equilibrium reactions. All equilibrium constants were taken from the WATEQ4F database (Ball and Nordstrom, 1991) with the exception of siderite, in which case log K was taken from the study by Bain et al. (2000). This equilibrium constant limits the extent of siderite precipitation in calcite-buffered systems and provides a potentially more realistic description, i.e. a limited attenuation of Fe(II) due to siderite precipitation.

The compositions of recharge water (surface infiltration), background (upgradient) groundwater, and initial tailings pore water are presented in Table 3, along with their source information. The recharge water is representative of rainwater with low total dissolved solids (TDS) and in equilibrium with atmospheric O_2 and CO_2. Major ion concentrations of rainwater are given by Appelo and Postma (1993), while arbitrarily low concentrations were assumed for heavy metals.

Table 1. Physical Input Parameters

Parameter	Symbol	Tailings Deposit				Eskerine Deposit	Source Information
		High S	Blended	Low S	Source Information		
soil classification		sandy silt, some clay	sandy silt, some clay	sand	Soil classification based on grain size distributions in NTC (1995, App. E.1).	gravelly sand	Soil classification based on grain size distribution envelope in Golder (1997; Fig. 11).
porosity [-]	q_s	0.50	0.50	0.50	Porosities based on dry bulk densities and gravimetric moisture contents in NTC (1995; Table 4).	0.30	Porosity is an assumed value.
hydraulic conductivity [m/s]	K_s	1.0E-07	1.0E-07	1.0E-07 4E-8 (below 25m depth)	Hydraulic conductivities based on bail testing of tailings piezometers FS15-B (piezo. tip 23m depth) and FS15-A (piezo. tip 34m depth) , in NTC (1995; Table 1).	3.0E-04	Hydraulic conductivity based on regional flow model-calibration results in Golder (1998a; Fig. 2.23) for Falconbridge Smelter Area, which included south half of Fault Lake Tailings Area.
residual moisture content [-]	θ_r	0.06	0.06	0.06	Unsaturated parameters (θ_r, α, n) adjusted to provide water saturations near 60 % in the vadose zone.	0.045	Unsaturated parameters (θ_r, α, n), based on typical values for sand (derived from the UNSODA database developed at the US Salinity Laboratory).
alpha [m^{-1}]	α	12.4	12.4	12.4		14.5	
fitting parameter [-]	n	3.7	3.7	3.7		2.68	
range in Infiltration [mm/yr]	I	250-580	NA	NA	Infiltration rate range from Golder (1996; pg 8; Table 3.5; Table 6.3).	450	Infiltration rate based on regional flow model-calibration results in Golder (1998a; Fig. 2.27).
Selected infiltration [mm/yr]	I	316	NA	NA	Model-calibrated value selected within range of potential infiltration rates reported by Golder (1996).	NA	

Table 2. Initial Mineralogical Composition

Reactive Mineral	Mineral Stoichiometry	Representative Mineral Volume Fractions (of Bulk Porous Medium)				Reactive Surface Area per 1L Bulk Porous Medium [m^2/L]		
		High S Tailings	Blended Tailings	Low S Tailings	Eskerine Aquifer	High S Tailings	Blended Tailings	Low S Tailings
Pyrrhotite	$Fe_{0.98}Ni_{0.02}S$	0.20	0.05	0.008	-	-	-	-
pentlandite	$Fe_{4.5}Ni_{4.5}S_8$	0.003	0.003	0.003	-	-	-	-
chalcopyrite	$CuFeS_2$	0.001	0.001	0.001	-	-	-	-
Calcite	$CaCO_3$	0.03	0.04	0.045	0.01	-	-	-
Anorthite	$CaAl_2Si_2O_8$	0.046	0.072	0.10	0.175	6.2	3.9	1.3
Biotite	$K(Mg_2Fe)(AlSi_3O_{10})(OH)_2$	0.013	0.026	0.04	0.01	1.7	1.4	0.5
Chlorite	$(Mg_4Fe_2)(4SiO_3)(OH)_4$	0.091	0.142	0.193	0.003	12.4	7.7	2.5

Mineral fractions for tailings estimated from elemental analysis and qualitative XRD analysis of tailings solids, in NTC (1995, Tables 13 and 14), as follows:

- Pyrrhotite content from total S wt%; pyrrhotite stoichiometry is assumed.
- Pentlandite content from residual Ni wt%, after satisfaction of the Ni content in pyrrhotite.
- Chalcopyrite content from total Cu concentration.

Calcite content of the Blended and Low S Tailings quantitatively estimated from neutralization potential results by NTC (1995, Table 21, Fig. 12c).

Calcite in the High S Tailings based on model-calibration to observed analytical results.

Reactive surface areas derived from median grain size (d50) of tailings, and assuming that the mineral grains are perfectly spherical.

Mineral fractions for eskerine deposit based on quantitative XRD analysis of native sediments from the East Tailings Area, in Golder (1998b)

Table 3. Initial Chemical Composition of Recharge Water, Background Groundwater, and Tailings Pore Water

Component	Recharge Water	Background Groundwater [1]		Initial Tailings Pore Water [2]	
		Field Data	Equilibrated*	Field Data	Equilibrated**
	[mol/L]	[mol/L]	[mol/L]	[mol/L]	[mol/L]
Ca	3.70E-07	9.20E-04	4.05E-03	4.35E-03	9.75E-04
K	1.00E-07	6.40E-05	3.89E-04	3.89E-04	6.40E-05
H_4SiO_4	1.00E-08	2.26E-04	1.64E-04	1.64E-04	2.26E-04
Al	1.00E-10	4.60E-06	3.42E-08	1.89E-05	1.98E-07
SO_4	7.70E-07	4.27E-04	5.73E-03	5.73E-03	4.27E-04
Alkalinity (eq/L)	-	1.60E-03	1.70E-03	5.40E-03	4.74E-03
CO_3	3.16E-04	-	5.62E-03	-	1.73E-03
pH	5.7	7.5	7	7.2	7.8
Eh [mV]	880	355	273	197	13
Fe^{2+}	1.00E-20	2.24E-07 (as Fe_{tot})	2.24E-07	2.24E-07 (as Fe_{tot})	1.11E-10
Fe^{3+}	1.00E-08	-	6.78E-12	-	2.55E-08
pO_2 (atm)	2.10E-01	-	1.00E-70	-	1.00E-40
pCO_2 (atm)	$10^{-3.5}$				
Ni^{2+}	1.00E-10	2.13E-07	2.18E-05	2.18E-05	2.13E-07
Cu^{2+}	1.00E-10	1.97E-07	8.84E-09	1.97E-07	1.97E-07
Mg	3.70E-07	6.40E-05	5.14E-04	5.14E-04	3.83E-04

1. Background chemistry from piezometer FS2-A (May 1994), in NTC (1995; Tables 6 and 9)
2. Initial tailings water chemistry from piezometer FS15-B (Aug 1994), in NTC (1995; Tables 7 and 10)

* equilibrated with calcite, amorphous Al-hydroxide, and amorphous ferrihydrite using PHREEQC at 25^0C

** equilibrated with calcite and amorphous Al-hydroxide using PHREEQC at 25^0C

The composition of background (regional) groundwater was estimated from analytical results of groundwater collected upgradient of the tailings area (piezometer FS2-A, NTC 1995) equilibrated with calcite, amorphous Al-hydroxide, and amorphous ferrihydrite using the PHREEQC speciation model. The initial composition of the tailings pore water at the time of deposition is unknown. Water chemistry from groundwater collected from the deep (unaltered) tailings environment (piezometer FS15-B; NTC 1995) equilibrated with calcite and amorphous Al-hydroxide was used for the initial pore water composition.

Domain and Boundary Conditions - 1D Vertical Simulations

The 1D simulation domain extended vertically from the top of the tailings, through the 30 m thick tailings deposit near its centre, and into the top 10 m of the eskerine aquifer. The spatial domain was subdivided into 85 finite-volume cells of varying sizes. Cell size increased gradually with depth and ranged from 0.1 m at the top to 1.25 m at the base. Small cells (10 cm length) were used for the near-surface tailings to adequately capture the location of the oxidation front.

The flow boundary conditions consist of a constant recharge flux at the top equivalent to the infiltration rate for High S Tailings (presented in Table 1), and a constant hydraulic head at the bottom which yields the average water table elevation within the tailings area (299 meters above mean sea level or masl). The transport boundary conditions consist of: a specified mass flux boundary condition at the top characterized by the composition of recharge water (Table 3) with a constant O_2 concentration equivalent to atmospheric, and a free exit boundary at the bottom.

Domain and Boundary Conditions -2D Cross-Sectional Simulation

The 2D simulation domain is a vertical cross-section through the tailings and overburden to the downgradient sensitive receptor northeast of the tailings area. The trajectory of the cross-section, which follows the observed groundwater flow path from the upgradient side of the tailings area to the nearest kettle lake, is presented in Fig. 2. A simplified schematic of the cross-section is presented in Fig. 3.

The 2D spatial domain was subdivided into approximately 4000 finite-volume cells of varying sizes. Similar to the 1D simulations, smaller cells (30 cm cells) were used to represent the near-surface tailings, and cell size gradually increased with depth. Also, a smaller horizontal discretization interval was used in the tailings area relative to the eskerine deposits to allow better delineation of the reaction front location while maintaining a minimal number of cells to minimize computational effort.

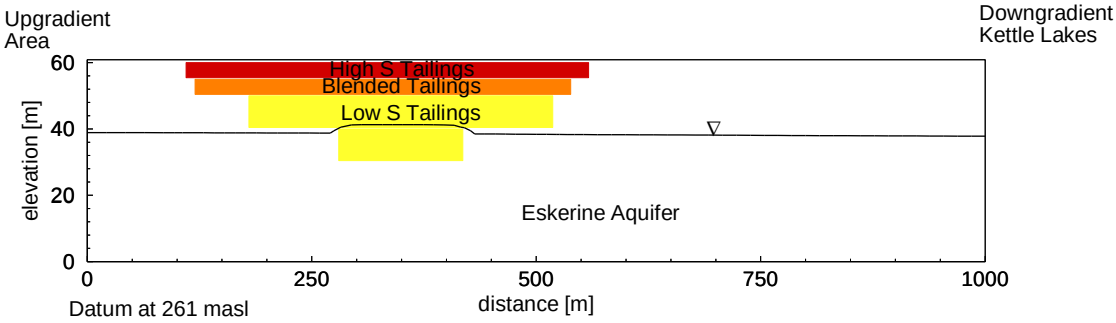

Figure 3: Schematics of the 2D Cross-Section

The flow boundary conditions consist of a constant recharge flux equivalent to the infiltration rate for the surficial material along the top boundary (presented in Table 1), constant hydraulic heads in the saturated zones of the left (head = 300.0 masl) and right (head = 298.9 masl) boundaries, which are equivalent to the local piezometric surface (see Fig. 3), and zero-flux conditions along the base and at the left and right boundary in the vadose zone. These conditions are based on the assumptions of predominately horizontal groundwater flow in the saturated zone, predominantly vertical groundwater flow in the vadose zone, and a relatively impermeable bedrock surface.

The transport boundary conditions consist of a constant mass flux along the top boundary characterized by the composition of recharge water (Table 3) with a constant O_2 concentration equivalent to atmospheric, a constant mass flux corresponding to the background groundwater in the saturated zone at the left (inflow) boundary, and a free-exit boundary in the saturated zone at the outflow. The remaining boundaries are assumed to have a zero mass flux.

Results and Discussion

1D Vertical Simulations

Observed tailings porewater chemistry data along a vertical profile through the approximate central area of the impoundment (from borehole FS15-A), collected by NTC (1995) in December 1993, and model-computed results for the 1D simulation at a run-time of 16 years, are presented in Fig. 4. The 16 years run-time represents the elapsed time from the cessation of tailings deposition in 1978, to when the tailings samples were collected and analyzed at the end of 1993. Modeling analysis focused on the unsaturated zone, where the assumption of vertical flow is reasonable. Given the uncertainties in the input parameters, there is good agreement between computed and observed oxygen partial pressures, pH-values, and concentrations of Fe^{+2}, SO_4^{-2}, Ca, and Al. This suggests that field conditions are reasonably well reproduced by the model on the whole, which supports the mechanisms and processes outlined in the conceptual model. Oxygen is consumed rapidly at shallow depth, and correlates well with a release of Fe, $SO_4^{-2}$and low pH.

The results indicate that after 16 years very little of the original sulfide minerals were oxidized, while calcite starts to become depleted near the ground surface. Calcium is controlled by equilibrium with calcite and/or gypsum, and dissolved Al is limited by equilibrium with amorphous Al-hydroxide. The results for Cu are not shown because field-measured (and simulated) Cu-concentrations were mostly below the analytical method detection limit. The discrepancy in Ni concentrations indicates that additional mechanisms for Ni attenuation exist, which are not considered by the model because they are difficult to quantify at present.

2D Cross-Sectional Simulation

Steady-State Flow Solution. The steady-state flow solution for the 2D simulation shows vertical percolation of infiltrating water through the unsaturated tailings and native sediments, which ultimately recharges the underlying unconfined aquifer (Fig. 5). The steady-state percolation velocities through the tailings and aquifer are 0.003 m/d (1 m/yr) and 0.04 m/d (15 m/yr), respectively. The percolation velocities are a function of the infiltration flux (316 mm/yr for tailings and 450 mm/yr for eskerine deposits) and the moisture content in the vadose zone (0.3 for the tailings and 0.03 for eskerine deposits).

Saturated groundwater flow is predominantly horizontal, with a linear flow velocity ranging from 0.05 to 0.14 m/d (20 to 50 m/yr) in the eskerine aquifer. The velocity increases in the direction of flow due to the increasing contribution of infiltrating water along the flow path. This is consistent with the configuration of the recharge area and the regional groundwater flow regime (Fig. 2).

A significant feature of the modeled flow regime is the deflection of upgradient groundwater below (and around, although not seen in 2D) the deep portion of the tailings mass which lies below the water table. This feature was termed the ‘porous envelope effect’ by NTC (1995) and is caused by the three order of magnitude permeability contrast between the saturated eskerine and saturated tailings deposits (see Table 1). As seen in Fig. 5, the porous envelope effect does not prevent AMD from impacting the aquifer because most of the tailing mass lies in the thick unsaturated zone where pore water migration is near vertical, thus AMD generated in the shallow tailings ultimately recharges the aquifer.

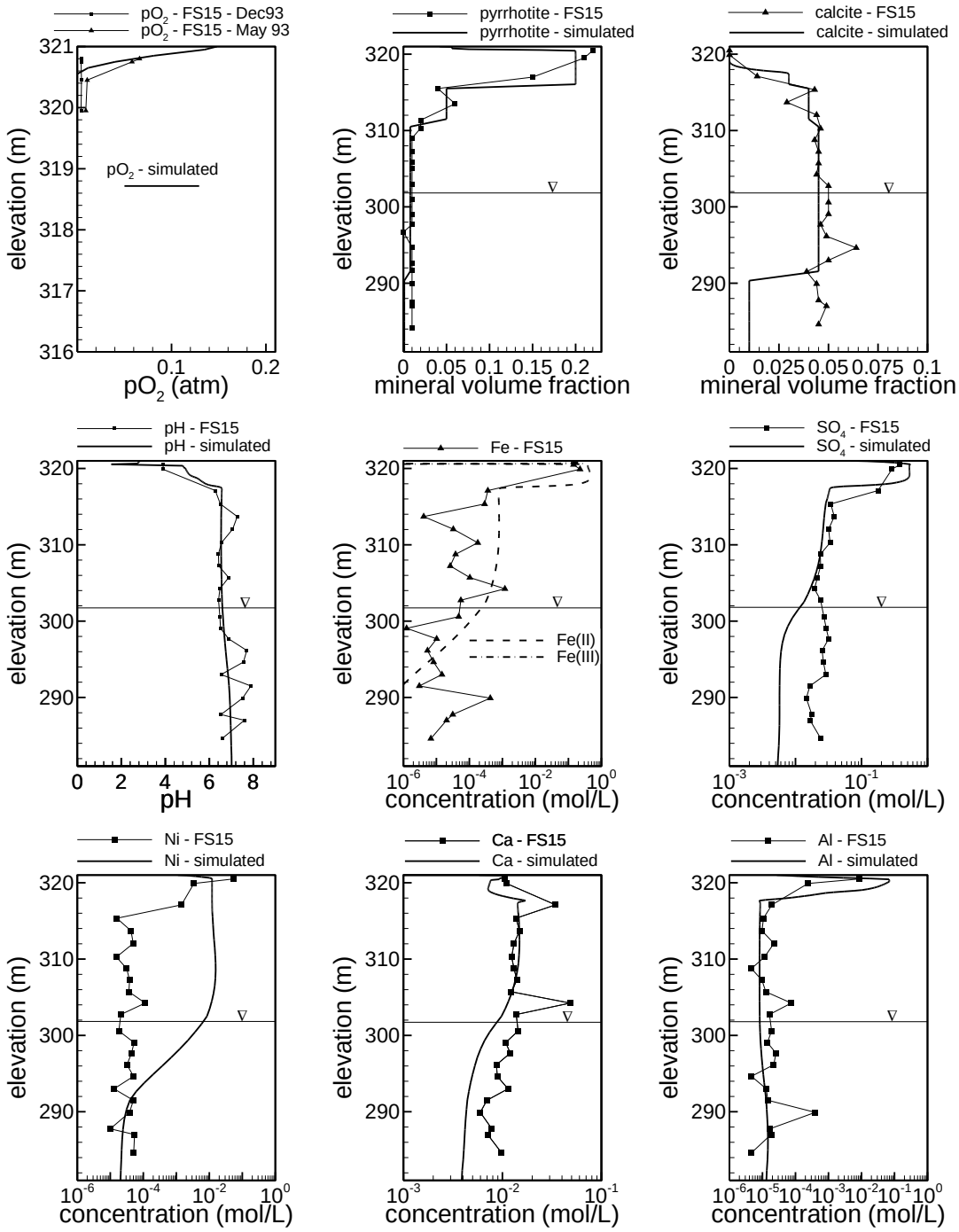

Figure 4: Comparison of observed and computed concentration distributions versus depth; T=16 years; field data: tailings from Borehole FS15-A, December 1993 (NTC 1995).

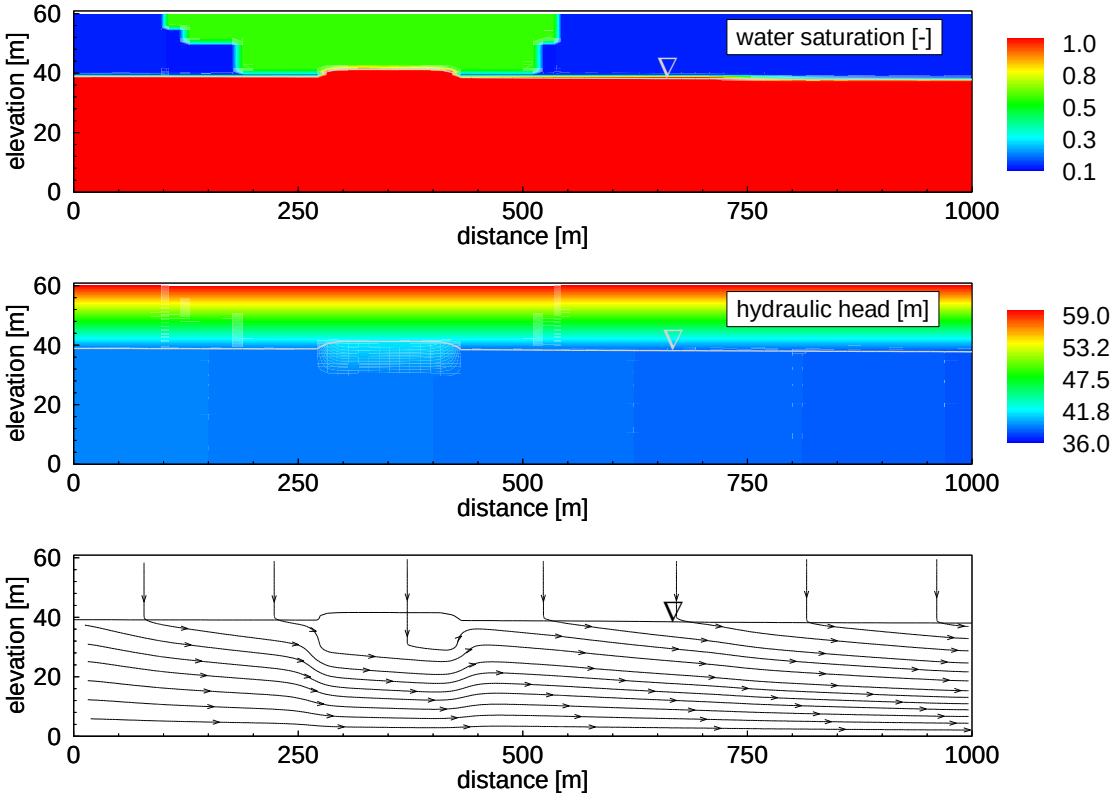

Figure 5: Steady-state saturations and groundwater flow regime

Reactive Transport Solution.

The volume fractions of key mineral phases in the subsurface after a simulation time of 1,000 years, are presented in Fig. 6. These results indicate that the top 3 m of tailings has been completely oxidized, as shown by the depletion of sulfide minerals (pyrrhotite, pentlandite, and chalcopyrite) in this zone. However, the 2 m of tailings below the oxidation front has still a high sulfide mineral content. The incomplete oxidation of the High S Tailings layer after 1,000 years implies a long term release potential of poor quality tailings drainage; however, the rate of release will be relatively low in comparison with earlier years, as is indicated by the decline in oxygen flux across the tailings ground surface over time (Fig. 7).

Within the oxidized tailings zone the results suggest ferrihydrite precipitation (Fig. 6), thus reducing Fe concentrations in this zone (Fig. 8) and potentially leading to the formation of a hardpan, although the reduced permeability caused by the hardpan formation is not considered by the model. The development of a hardpan was observed in the field by NTC (1995). Formation of a hardpan may retard the flux of O_2 into the tailings and, consequently, limit oxidation of the tailings. Near the oxidation front, covellite precipitates (Fig. 6), controlling dissolved Cu concentrations immediately below the oxidation front (Fig. 8). In the field, attenuation of Cu will primarily depend on pH and the availability of dissolved sulfide. The tailings are significantly depleted in calcite at this stage, except for a small, hydraulically isolated zone (i.e., upgradient saturated groundwater flow tends to circumvent this area) at the base of the

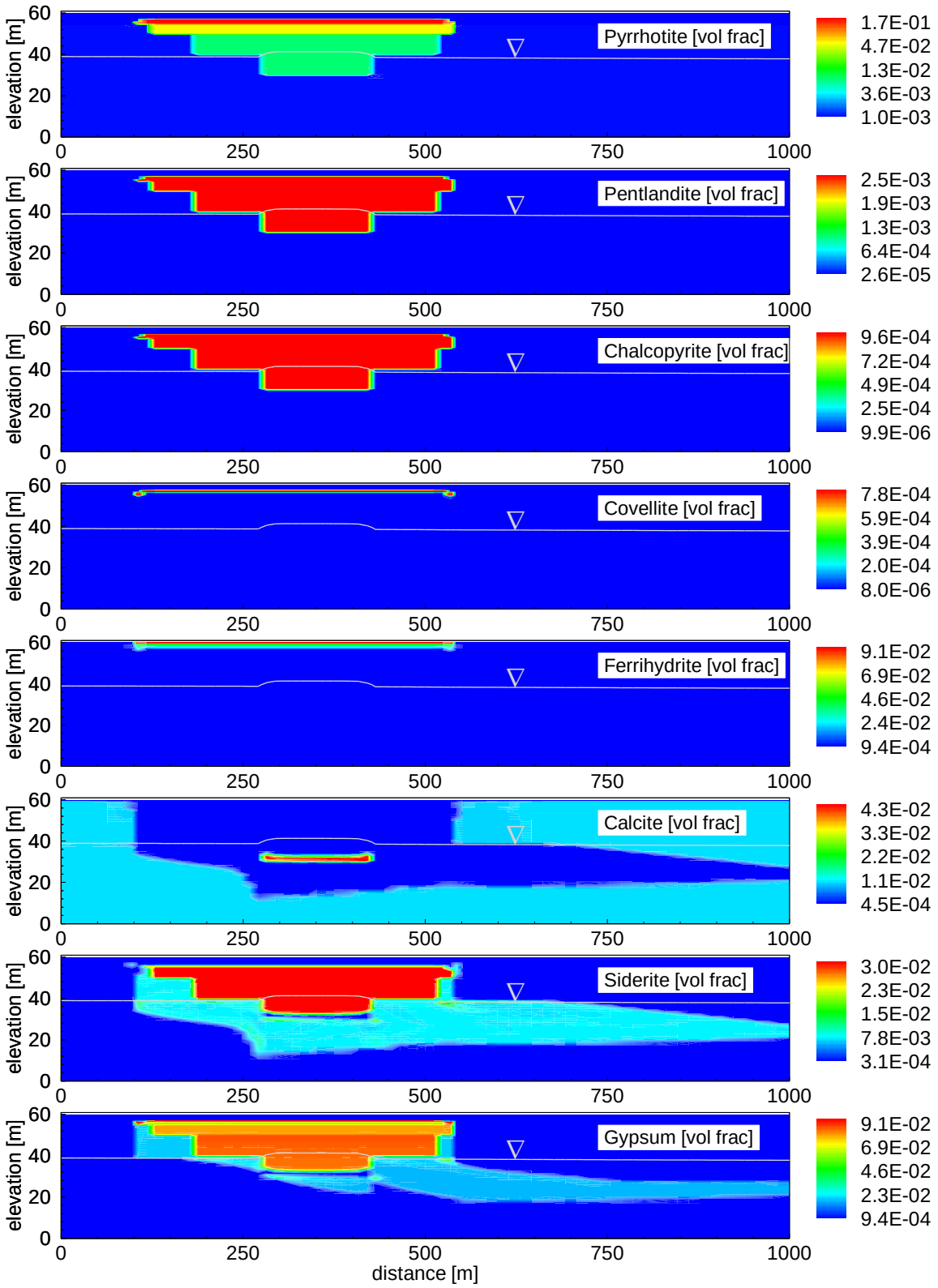

Figure 6: Volume fractions of key mineral phases; T=1,000 years

thickest area of the tailings (Fig. 6). As a result, the pH-buffering capacity of the tailings below the water table may have a limited effect on improving drainage water quality, considering that AMD-impacted recharge water which has entered the saturated zone tends to circumvent this zone. The 2D simulation further indicates that the area of the aquifer which has contacted the tailings plume is also depleted in calcite, and gypsum and siderite have formed in the calcite-depleted zones. Most importantly, the simulations suggest that after 1,000 years, the zone of calcite depletion extends to the downgradient receptor, the nearest kettle lake.

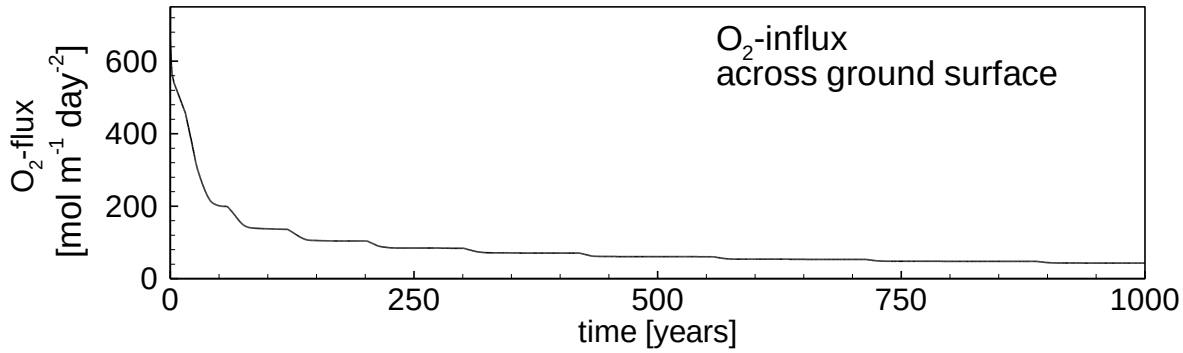

Figure 7: Transient evolution of O_2 flux across the tailings ground surface.

The tailings plume migrates laterally from around and below the saturated tailings mass and extends to the nearest kettle lake (Fig. 8). The plume is characterized by a sub-neutral pH, elevated concentrations of Fe, SO_4, and Ca, and low alkalinity, relative to background groundwater. Elevated Cu and Al concentrations (Fig. 8) exist in the unsaturated tailings near to the oxidation front, but are significantly attenuated by the precipitation of covellite and amorphous aluminum hydroxide, respectively (Fig. 6). Elevated Ni concentrations exist throughout the unoxidized tailings. This is because the nickel hydroxide [$Ni(OH)_2$] mineral phase remains undersaturated throughout the tailings, and other potential attenuating mechanisms for Ni have not been considered by the model.

Within the deepest zone of the tailings, where calcite is still present, the concentration of the plume constituents, other than Ca, have remained low, and pH and alkalinity are near background levels (Fig. 8), due to pH buffering by calcite. However, where the vertical extent of the tailings is limited to the vadose zone, low quality tailings drainage enters the underlying aquifer. The generation of AMD in the unsaturated tailings is similar everywhere (regardless of the depth of the tailings); the only difference is that regions underlain by thicker tailings possess a greater buffering capacity per tailings area, hence the resultant basal seepage has a better quality for a longer period of time. This implies that the thin areas of the tailings, i.e. the peripheral zones of the Fault Lake Tailings Area, are more likely to generate poor quality drainage rather than the thicker tailings situated in the center of the Fault Lake basin. This result is primarily due to the contrasting (higher) calcite content of the unoxidized tailings relative to the surrounding eskerine deposits (Table 2).

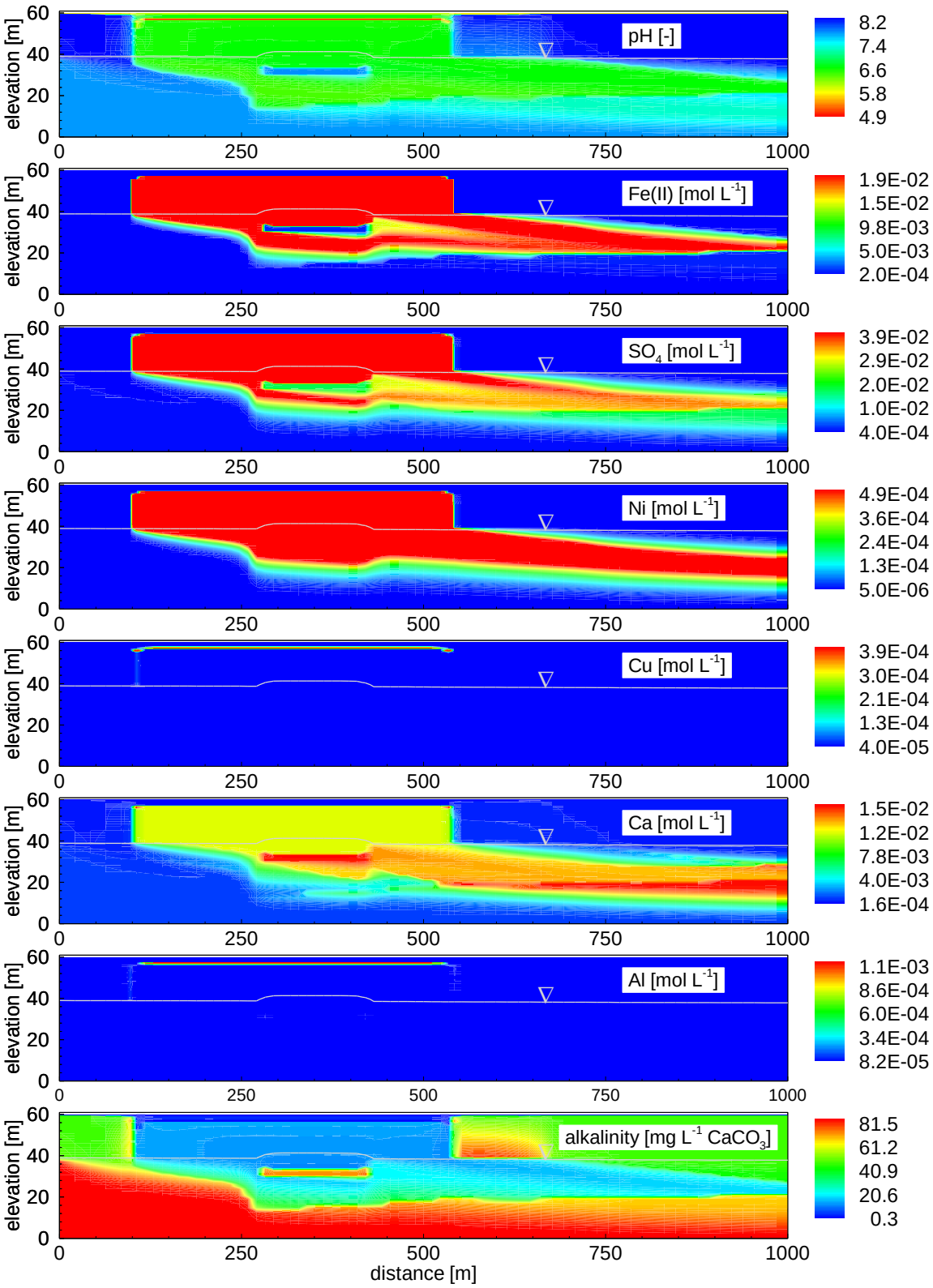

Figure 8: Aqueous concentrations of key species; T=1,000 years

It has to be recognized that the calcite content of the tailings (approx. 3 to 4.5 vol. %) is a poorly constrained parameter. If the calcite content is actually lower than this estimate, drainage with low pH and high concentrations of heavy metals and SO_4^{-2} will recharge the aquifer at an earlier time than simulated.

Mass Loading and Peak Concentrations at the Sensitive Receptor

The predicted cumulative mass loading curves and depth-integrated discharge concentrations at the sensitive receptor for the constituents of interest are presented in Fig. 9. In general, the mass loading of Fe, SO_4^{-2}, and Cu increase fairly linearly over most of the 1,000-year simulation period. A potentially significant result is that elevated Fe-discharge to the receptor is not expected for many centuries; simulated Fe-loadings do not increase significantly before 950 years.

The linear increase in mass loading is caused by the assumed equilibrium conditions with respect to siderite, gypsum, and covellite in the presence of calcite, which maintains relatively constant dissolved Fe, SO_4^{-2}, and Cu concentrations (Fig. 9). The marked increase in mass loading and concentration of Fe after 950 years indicates the point in time when calcite is fully consumed in the tailings and aquifer along the flow path of the tailings plume.

Model Uncertainties and Data Gaps

It is important to note that if siderite and covellite do not precipitate to the simulated extent, the cumulative mass loading for Fe and Cu may be higher. If the carbonate content of the tailings or the aquifer is lower than in the simulations, the pronounced increases in the loading rates/concentrations may occur earlier. It should also be recognized that a number of poorly constrained and interconnected physical parameters, including recharge rate, hydraulic conductivity, unsaturated soil hydraulic function parameters, and moisture content, can also significantly affect the model results. As indicated previously, water saturation in the unsaturated tailings is considered to be the most crucial physical parameter affecting the potential for the release of acidity and metals from the tailings, because the ingress of atmospheric oxygen increases strongly with decreasing moisture content.

Several key information gaps have been identified by this study that, if resolved, would improve/qualify the conceptual model, reduce the uncertainty in the model predictions, and refine estimates of the potential for impact to the surrounding environment. For example, a detailed quantitative mineralogical analysis of the tailings solids along their vertical extent through the unsaturated tailings would allow an evaluation of sulfide mineral stoichiometry (as an indicator for the potential for acid production by pyrrhotite oxidation by O_2); the presence of secondary Cu-sulfide mineral phase such as covellite (to confirmation the potential for Cu attenuation); the composition of hydroxides (to determine the potential for Ni attenuation by co-precipitation with ferrihydrite); the existence of siderite precipitation (as a major attenuation mechanism for dissolved Fe^{+2}); and calcite content (as the major pH-buffering mineral phase). In addition, field-measured volumetric moisture content and porosity data for the tailings over their vertical extent in the vadose zone would be useful for constraining the model results.

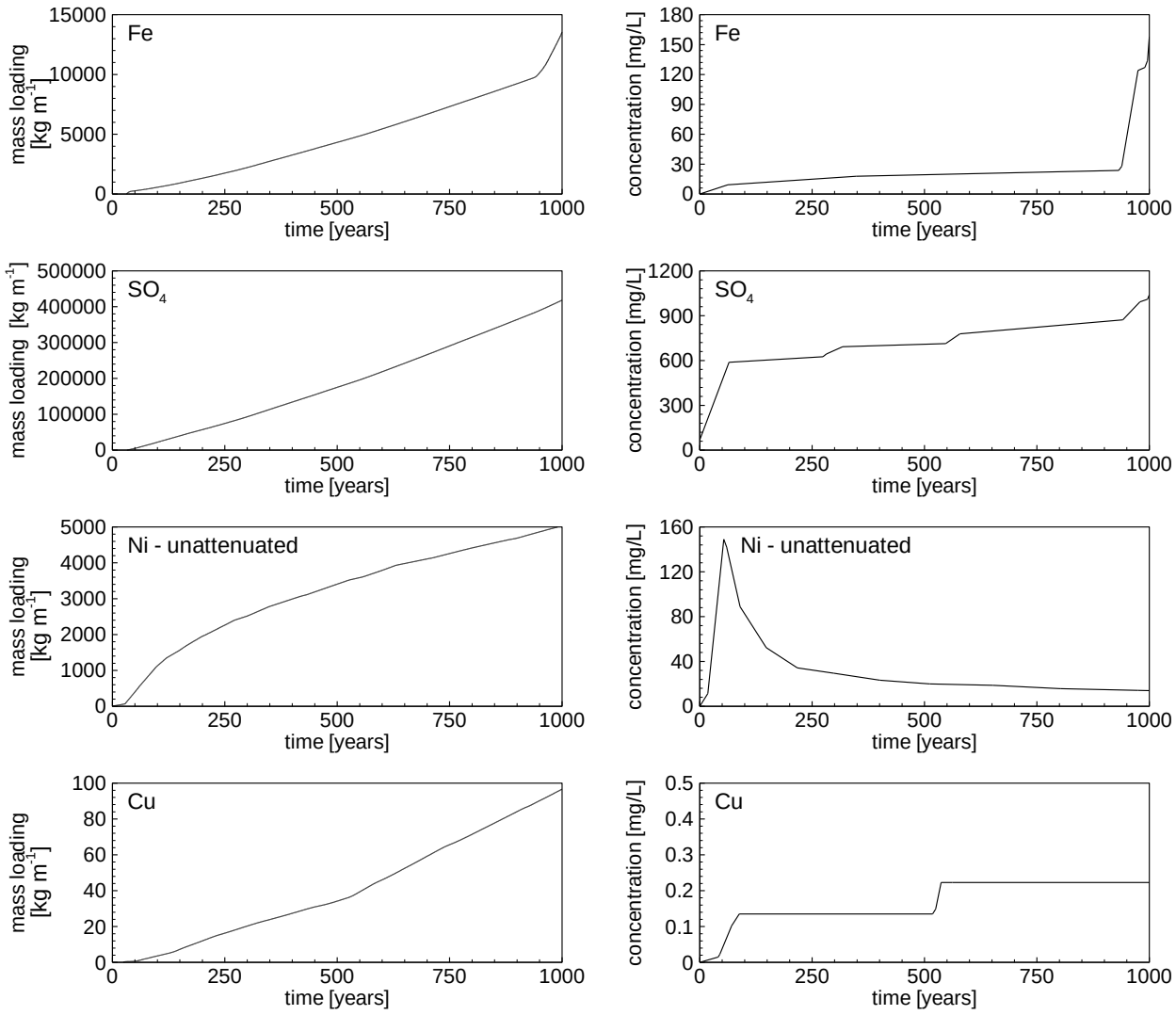

Figure 9: Mass loading and depth-integrated concentration breakthrough of components of interest at the nearest kettle lakes.

Summary and Conclusions

Through numerical simulation, the spatial distributions of key physical, hydrogeological and geochemical characteristics of the Fault Lake Tailings Area (i.e., permeability contrast, impoundment geometry, mineralogy, and variable saturation) are seen to significantly affect the manner in which the tailings impact the surrounding environment. The main conclusions of this study are summarized below, along with the key characteristics associated with these conclusions:

- Only the top three meters of tailings are estimated to become fully oxidized. Therefore, the remaining portion of the High Sulfide Tailings layer can potentially remain unoxidized over the long term. This implies a long term release potential of poor quality tailings drainage; however, the rate of release will be much lower in comparison with earlier years.

- A significant feature of the groundwater flow regime is the deflection of upgradient groundwater around the deep portion of the tailings mass which lies below the water table. However, this effect, caused by contrasting permeability between the saturated tailings and the native sediments, does not prevent AMD generated in the shallow unsaturated tailings environment from directly percolating into the aquifer.
- Although counter-intuitive, the thin areas of the tailings at the periphery of the impoundment are more likely to generate poor quality drainage than the thicker tailings areas situated centrally in the Fault Lake basin. This is primarily due to the contrasting (higher) calcite content of the unoxidized tailings relative to the underlying eskerine deposits.
- The groundwater plume is predicted to be characterized by a sub-neutral pH, elevated concentrations of Fe, SO_4^{-2} Ni, and Ca, and low alkalinity, relative to background groundwater. Elevated Cu and Al concentrations exist in the unsaturated tailings near to the oxidation front, but are potentially attenuated by the precipitation of covellite and amorphous $Al(OH)_3$, respectively. Field data suggest that mechanisms for Ni attenuation exist, but remain unknown, and therefore none were considered in this study.
- Over the long term, the tailings and the area of the aquifer which has been affected by the tailings plume will potentially be depleted in calcite. This zone of calcite depletion possibly can extend to the downgradient receptor, the nearest kettle lakes. However, the results suggest that pore water containing high Fe-concentrations will not reach the receptor for several centuries.

This study serves as a useful example of the strength and limitations of multi-component reactive transport modeling. The simulations provide additional insight into the anticipated fate of AMD released from the tailings, particularly by considering the spatial complexity of the site, hydraulic conductivity contrasts, varying mineralogical composition of the tailings layers and the aquifer, and by taking into account unsaturated and saturated conditions in the tailings and aquifer. The arrival of elevated major ion concentrations in groundwater at the sensitive receptor (SO_4^{-2}, Ca) is considered to be reasonably well predicted by this study, given the assumptions made in the conceptual model and the simple geochemistry associated with major ions; i.e. solubility control by rapidly reacting mineral phases such as calcite, gypsum, and ferrihydrite. However, the arrival of elevated trace/heavy metals concentrations is likely over-predicted because of the high degree of uncertainty in the geochemical data available, and because the processes affecting metals mobility are too complex and also highly uncertain. This study included some attenuating reactions for trace/heavy metals (covellite precipitation), however, more may exist which may further reduce metal concentrations in groundwater downgradient of the Fault Lake Tailings Area. It can also be envisioned that attenuation is less significant than predicted, for example due to the formation of surface coatings on buffering minerals and the existence of preferential flow paths.

Acknowledgements

We sincerely appreciate Marc Butler of Falconbridge Limited for his support of this study and his encouragement towards the production of this paper. We would also like to thank Nicki McKay of NTC for her invaluable assistance with the estimation of the mineralogical composition of the Fault Lake Tailings.

Table 1. Physical Input Parameters

References

Amos, R. T., Mayer, K. U., Blowes, D. W., and Ptacek, C. J., 2004. Reactive transport modeling of column experiments for the remediation of acid mine drainage, Env. Sci. Technol., 38:3131-3138. http://dx.doi.org/10.1021/es0349608.

Appelo, C.A.J., and Postma, D., 1993. Geochemistry, groundwater and pollution. A.A. Balkema, Rotterdam, Netherlands.

Bain, J.G., Blowes D.W., Robertson, W.D., and Frind, E.O., 2000. Modelling of sulfide oxidation with reactive transport at a mine drainage site. J. Contam. Hydrol. 41, 23-47. http://dx.doi.org/10.1016/S0169-7722(99)00069-8.

Ball, J. W., Nordstrom, D. K., 1991. User's Manual for WATEQ4F, with revised thermodynamic database and test cases for calculating speciation of major, trace and redox elements in natural waters. U.S. Geological Survey, Open File Report 91-183, 189pp.

Golder 1997. Updated Hydrogeology; Falconbridge Smelter Area; Falconbridge, Ontario. January 1997. Report No. 961-1823A

Golder 1996. Closure Plan; Fault Lake Tailings Area; Falconbridge, Ontario. November 1996. Report No. 951-1847/6000.

Golder 1998a. Hydrogeological Assessment; Closure Plan – Falconbridge Smelter Area. December 1998. Report No. 961-1847/5632.

Golder 1998b. Closure Plan – Falconbridge Smelter Area. December 1998. Report No. 961-1847/6210.

Johnson, R.H., Blowes, D.W., Robertson, W.D., and Jambor, J.L., 2000. The hydrogeochemistry of Nickel Rim mine tailings impoundment, Sudbury, Ontario. J. Contam. Hydrol. 41, 49-80. http://dx.doi.org/10.1016/S0169-7722(99)00068-6.

Jurjovec, J., Blowes, D. W., Ptacek, C. J., and Mayer, K. U., 2004, Multicomponent reactive transport modelling of acid neutralization reactions in mill tailings. Water Resour Res., 40, W11202, doi:10.1029/2003WR002233. http://dx.doi.org/10.1029/2003WR002233.

Mayer, K. U., Blowes, D. W., and Frind, E. O., 2000. Numerical Modeling of acid mine drainage generation and subsequent reactive transport. ICARD 2000, Proceedings from the Fifth International Conference on Acid Rock Drainage, Sponsored by the Society of Economic Geologists, Denver, Colorado, May 21-24,Vol. 1, 135-142.

Mayer, K. U., Benner S. G., and Blowes, D. W., 1999. The reactive transport model MIN3P: Application to acid mine drainage generation and treatment - Nickel Rim Mine Site, Sudbury Ontario. In: Sudbury '99 Mining and the Environment II Conference Proceedings. Eds. D.Goldsack, N. Belzile, P. Yearwood and G. Hall. September 13-17, 1999, Sudbury, Ontario. p.145-154.

Mayer, K. U., Frind, E. O., and Blowes, D. W., 2002. Multicomponent reactive transport modeling in variably saturated porous media using a generalized formulation for kinetically controlled reactions, *Water Resour. Res.*, 38, 1174, doi: 10:1029/2001WR000862.

NTC, 1995. Investigation of the Porous Envelope Effect at the Fault Lake Tailings Site. Noranda Technology Centre. May 1995. Golder Reference No. 951-1847.